cosmetics

MDPI

Article

A Thermostable Aspartic Protease from Bitter Melon (*Momordica charantia*) as a Novel Cosmetic Enzyme for Skin Exfoliation and Hydration: Enzymatic Stability and Pilot In-Use Skin Benefits

Somi Park *, Ji Eun Lee, Hee Cheol Kang and Jin Woo Min *

Green & Biome Customizing Laboratory, GFC Life Science Co., Ltd., Hwaseong 18471, Republic of Korea
* Correspondence: sm.park1@gfcos.co.kr (S.P.); jw.min@gfcos.co.kr (J.W.M.); Tel.: +82-10-5364-2976 (S.P.); Fax: +82-31-5183-5519 (S.P.)

Abstract

Naturally derived cosmetic enzymes from food-grade plant sources are increasingly sought after as sustainable and skin-compatible alternatives to conventional exfoliating agents; however, many existing plant proteases exhibit poor thermal stability, limiting their practical use in cosmetic formulations. In this study, a thermostable keratinolytic protease extracted from *Momordica charantia* (bitter melon), a widely consumed edible and medicinal plant, was characterized to overcome these limitations and evaluated for its cosmetic applicability. The enzyme demonstrated strong keratin-degrading activity and retained over 80% of its activity at 70 °C, indicating superior thermal stability compared with commonly used cosmetic enzymes. In vitro assays using RAW264.7 murine macrophages confirmed low cytotoxicity and revealed significant inhibition of lipopolysaccharide-induced nitric oxide production, along with moderate elastase inhibitory activity, suggesting additional skin-beneficial properties. To assess practical exfoliating efficacy and skin compatibility, a four-week in-use test was conducted with 11 healthy adult volunteers using a formulation containing the *M. charantia*-derived enzyme. Significant reductions in desquamation index and improvements in skin smoothness (SEsm), measured using a Visioscan® VC20 Plus, and hydration, assessed with a Corneometer® CM825, were observed ($p < 0.001$), with no adverse effects reported. Collectively, these findings indicate that this naturally sourced, plant-derived keratinase offers a thermally stable and effective enzymatic exfoliation strategy, supporting its potential use as a sustainable cosmetic bioactive ingredient.

Keywords: bitter melon (*Momordica charantia*); keratinolytic enzyme; enzymatic exfoliation; thermal stability; cosmetic enzymes; in-use test; skin hydration

Check for updates

Academic Editors: Enzo Berardesca and Antonio Vassallo

Received: 5 January 2026
Revised: 27 January 2026
Accepted: 9 February 2026
Published: 11 February 2026

Copyright: © 2026 by the authors. Licensee MDPI, Basel, Switzerland. This article is an open access article distributed under the terms and conditions of the Creative Commons Attribution (CC BY) license.

1. Introduction

The stratum corneum, the outermost layer of human skin, is composed primarily of keratin-rich corneocytes that accumulate over time, leading to a rough texture and dull appearance [1]. These corneocytes originate from basal keratinocytes that undergo a stepwise differentiation process as they migrate toward the skin surface. Under normal conditions, old corneocytes are naturally removed and replaced by newly formed cells [1]. However, factors such as aging, environmental stress, hormonal imbalance, and certain skin conditions can impair this renewal process, resulting in excessive keratin buildup [2–4].

As a result, the skin surface often becomes dry and uneven, which can also reduce the effectiveness of topical treatments.

To address this issue, exfoliating agents are widely employed to promote the removal of accumulated keratin [2]. Alpha hydroxy acids (AHAs) and beta hydroxy acids (BHAs) are commonly used chemical exfoliants [5,6], but their low pH and mechanism of action can trigger skin irritation, particularly in individuals with sensitive skin [7,8]. As a gentler alternative, enzymatic exfoliation using proteolytic enzymes has garnered increasing attention [9]. Keratinases—enzymes that degrade the insoluble protein keratin—offer an effective yet mild approach to exfoliation [9–11]. However, many naturally derived proteases lack the thermal and formulation stability required for cosmetic applications [12]. Furthermore, commercially available enzymes often rely on imported botanical sources, such as papain [13] from papaya, which may suffer from reduced activity during processing and storage [14].

Bitter melon (*Momordica charantia*, BM) is a plant traditionally used in herbal medicine across Asia, Africa, and the Caribbean [15–19]. It has been reported to exhibit a range of pharmacological effects, including antioxidant, anti-inflammatory, antidiabetic, anticancer, and antimicrobial activities [20–22]. More recently, studies have highlighted its potential dermatological applications, such as skin whitening, wound healing, and anti-aging effects [23,24]. Despite these benefits, its incorporation into cosmetic formulations—particularly in the context of proteolytic enzymes—remains underexplored. Proteolytic enzymes extracted from bitter melon have demonstrated substrate specificity, with a protease isolated from its seeds exhibiting notable stability and activity under physiologically relevant conditions [25]. These findings support the feasibility of utilizing bitter melon–derived enzymes in topical applications aimed at protein degradation, such as keratin removal.

In this study, we investigated the cosmetic potential of a keratin-degrading enzyme derived from bitter melon fruit, with particular emphasis on overcoming the stability limitations of conventional cosmetic proteases. The enzyme solution was biochemically characterized, with a focus on keratinolytic activity and thermal stability, and its performance was compared to that of papain. To assess its practical applicability, an in-use trial was conducted involving application of the enzyme solution to human skin. Evaluation metrics included keratin removal, improvement in skin texture, and hydration. The results supported the potential of the bitter melon–derived enzyme as a functional cosmetic ingredient for mild exfoliation and skin conditioning.

2. Materials and Methods

2.1. Materials

Fresh bitter melon (*Momordica charantia*), papaya (*Carica papaya*), and date palm (*Phoenix dactylifera*) fruits were obtained from a local agricultural market in Korea and used as enzyme sources. Sodium phosphate buffer (SPB), ammonium sulfate, keratin azure, papain, EDTA disodium salt dihydrate, E-64, N-succinyl-Ala-Ala-Ala-p-nitroanilide (SANA), lipopolysaccharide (LPS), oleanolic acid (used as a reference standard for elastase inhibition assay), and all other analytical-grade reagents were purchased from Sigma-Aldrich (St. Louis, MO, USA), unless otherwise stated.

Bicinchoninic Acid (BCA) protein assay kit, Bradford reagent, and Quick Start™ Bovine Serum Albumin (BSA) standards were purchased from Bio-Rad (Hercules, CA, USA). Sodium nitrite, used for the construction of the standard calibration curve in the nitric oxide (NO) assay, was obtained from Sigma-Aldrich (St. Louis, MO, USA).

Pepstatin A was obtained from Santa Cruz Biotechnology (Dallas, TX, USA). Dialysis tubing (Spectra/Por®, molecular weight cutoff 8 kDa) was purchased from Repligen

Corporation (Waltham, MA, USA). Keratin azure, used as the substrate for keratinolytic activity assays, was supplied by Sigma-Aldrich (St. Louis, MO, USA).

RAW 264.7 murine macrophage cells were obtained from the Korean Cell Line Bank (KCLB, Seoul, Republic of Korea). Dulbecco's Modified Eagle's Medium (DMEM), fetal bovine serum (FBS), and penicillin/streptomycin were purchased from HyClone (Logan, UT, USA) and Thermo Fisher Scientific (Waltham, MA, USA). The NO Plus Detection Kit was obtained from iNtRON Biotechnology (Seongnam, Republic of Korea), and the EZ-CytoX cell viability assay kit was purchased from DoGenBio Co., Ltd. (Seoul, Republic of Korea).

All solutions were prepared using distilled or triple-distilled water, and all reagents were used without further purification.

2.2. Preparation of Bitter Melon-Derived Keratinase Solution

Fresh bitter melon (*Momordica charantia*, BM) fruits (100 g) were used as the starting material. Seeds were removed prior to processing, while the pulp was retained. The plant material was homogenized in cold sodium phosphate buffer (SPB, 100 mM, pH 7.0; Sigma-Aldrich, St. Louis, MO, USA) at a ratio of 1:2 (*w*/*v*) using a blender. Homogenation was performed for 1 min per cycle for a total of three cycles, with the sample kept on ice between cycles.

The homogenate was filtered through sterile laboratory-grade gauze (300 mesh) to remove insoluble debris and subsequently centrifuged at 8000× *g* for 30 min at 4 °C to obtain the crude enzyme extract. The supernatant (approximately 200 mL) was collected and subjected to protein precipitation by adding ammonium sulfate (Sigma-Aldrich, St. Louis, MO, USA) to 80% saturation. Ammonium sulfate was added as an aqueous solution in a single step, followed by gently stirring at 4 °C for 12 h.

The resulting precipitate was collected by centrifugation (10,000× *g*, 30 min, 4 °C) and resuspended in 20 mL of SPB. The resuspended enzyme solution was subsequently dialyzed using Spectra/Por® dialysis tubing (molecular weight cutoff: 8 kDa; Repligen Corporation, Waltham, MA, USA) against 300 mL of SPB at room temperature. Dialysis was performed for 24 h with three buffer changes.

Following dialysis, the retained solution inside the dialysis tubing was collected and frozen at −80 °C prior to lyophilization. Freeze-drying was conducted for 24 h to obtain a dry enzyme powder.

For experimental use, the lyophilized enzyme was reconstituted in SPB to a final concentration of 10 mg/mL. Identical procedures were applied to prepare comparative enzyme solutions from papaya (*Carica papaya*, CP) and date palm (*Phoenix dactylifera*, PD).

2.3. Protein Quantification

Protein concentration was determined using both the Bicinchoninic Acid (BCA) and Bradford protein assay methods [26,27] to standard colorimetric protocols. Both assays were performed in triplicate using a microplate format, and absorbance was measured at 595 nm using a microplate reader (BioTek Instruments, Winooski, VT, USA). A standard calibration curve was generated using Quick Start™ Bovine Serum Albumin (BSA) standards (0–2.0 mg/mL; Bio-Rad, Hercules, CA, USA), and protein concentrations were calculated from the corresponding standard curves. The calibration curve ($y = 0.3031x + 0.0997$, $R^2 = 0.9799$) showed good linearity over the range of 0–2.0 mg/mL. The calculated LOD and LOQ were 0.031 mg/mL and 0.092 mg/mL, respectively.

2.4. Keratinolytic Activity Assay

Keratinolytic activity was assessed using keratin azure (Sigma-Aldrich, St. Louis, MO, USA) as the substrate. Keratin azure was rinsed thoroughly with distilled water to

remove impurities and dried at 40 °C for 24 h prior to use. Dried keratin azure (5 mg) was suspended in 10 mL of enzyme solution at a final concentration of 10 mg/mL. The reaction mixture was incubated at 37 °C for up to 5 days in sealed polypropylene tubes to prevent evaporation and contamination. After incubation, samples were centrifuged at 4000× *g*, 10 min, and the supernatants were filtered through a 0.45 µm membrane filter (ADVANTEC, Tokyo, Japan). The absorbance of the clarified supernatant was measured at 595 nm using a microplate reader (BioTek Instruments, Winooski, VT, USA). Increased absorbance indicated as an indicator of keratin degradation.

2.5. Effects of Temperature and pH in the Keratinolytic Activities

To evaluate the effect of temperature on keratinolytic activity, enzyme solutions (10 mg/mL, 10 mL) were incubated with keratin azure (5 mg) at 25 °C, 37 °C, 50 °C, and 70 °C for 5 days. Residual keratinolytic activity was quantified using the keratin azure assay described in Section 2.3 and expressed as a percentage of maximum activity observed under optimal conditions (Figure 1C).

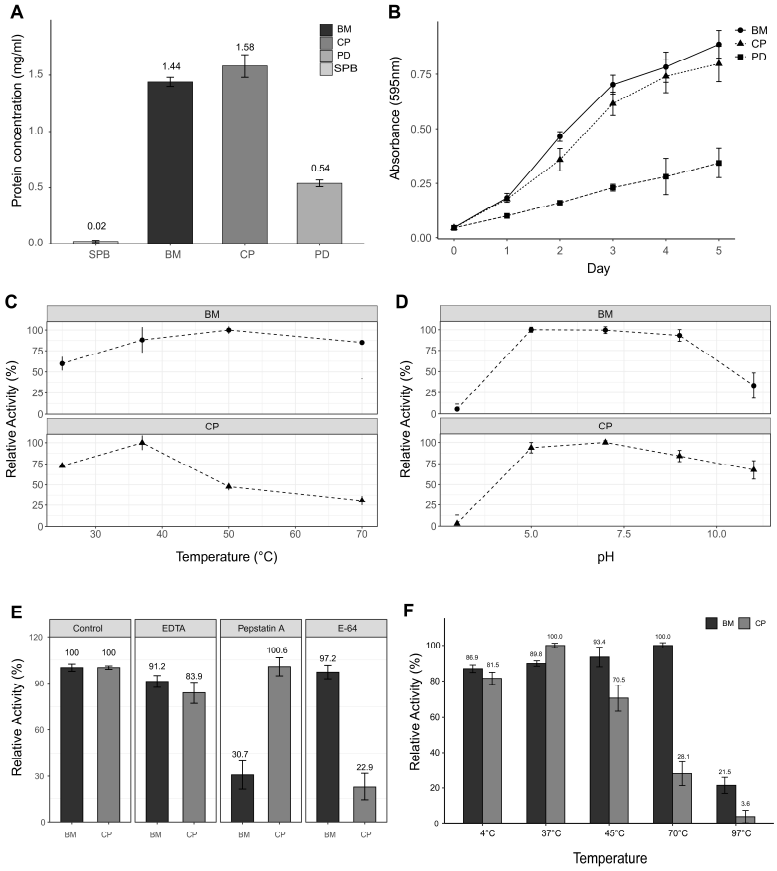


Figure 1. Biochemical characterization of bitter melon–derived keratinase in comparison with plant-derived comparators. (**A**) Protein concentrations of crude enzyme extracts obtained from bitter melon (BM), papaya (CP), and date palm (PD). (**B**) Keratinolytic activity of each extract, determined by absorbance at 595 nm following a 5-day incubation with keratin azure (pH 7.0, 37 °C), using equal protein amounts. (**C**) Thermal stability of enzyme solutions derived from BM and CP after incubation at varying temperatures for 5 days. (**D**) pH stability of BM and CP enzymes following 5-day incubation under a range of pH conditions. (**E**) Inhibitory effects of selected protease inhibitors (10 µM EDTA, 1 µM pepstatin A, and 3.7 µM E-64) on the keratin-degrading activity of BM and CP enzymes. All activity values were normalized to the control (no inhibitor), set at 100%. (**F**) Short-term thermal stability of BM-derived enzyme and papain after 1 h heat treatment. Activities were normalized to untreated controls (set to 100%). Data are presented as mean ± SD (n = 3). Statistical significance was evaluated using Student's t-test ($p < 0.001$).

To assay pH stability, enzyme solution (10 mg/mL, 10 mL) was assessed by incubating enzyme solutions in buffer systems ranging from pH 5.0 to 11.0 for 5 days. The following buffers were used: sodium acetate buffer (100 mM, pH 5.0), sodium phosphate buffer (100 mM, pH 6.0–8.0), Tris–HCl buffer (100 mM, pH 9.0), and glycine–NaOH buffer (100 mM, pH 10.0–11.0). Residual activity was determined using the keratin azure assay and compared to the activity at pH 7.0 and 37 °C (Figure 1D).

For thermal stability test, enzyme solutions (10 mg/mL) were pre-incubated without substrate at 4 °C, 37 °C, 45 °C, 70 °C, and 90 °C for 1 h. Samples were then cooled on ice for 10 min to terminate thermal exposure and equilibrate the temperature. Subsequently, keratin azure was added (5 mg in 10 mL reaction volume), and the reaction mixtures were incubated at 37 °C (Figure 1F). Residual enzymatic activity was measured and normalized to the control. Activities were normalized to untreated controls (set to 100%).

2.6. Protease Inhibition Assays

To determine the protease type of BM-derived keratinase, inhibition assays were performed using class-specific inhibitors (Figure 1E): Pepstatin A (aspartic protease inhibitor) [28], EDTA (metalloprotease inhibitor) [29], and E-64 (cysteine protease inhibitor) [30]. Papain (10 μg/mL; Sigma-Aldrich, St. Louis, MO, USA) was used as a reference enzyme.

Pepstatin A (Santa Cruz Biotechnology, Dallas, TX, USA) was dissolved in DMSO (Sigma-Aldrich, St. Louis, MO, USA) to prepare a 10 mM stock solution, then diluted with distilled water to a final concentration of 1 μM. EDTA disodium salt dihydrate (Sigma-Aldrich, St. Louis, MO, USA) was prepared in distilled water at 10 μM. E-64 (Sigma-Aldrich, St. Louis, MO, USA) was dissolved in DMSO to 1 mg/mL and diluted to 3.7 μM. For inhibition assays, inhibitors were added to the enzyme solutions at a volume of 100 μL per 10 mL reaction mixture, followed by pre-incubation at 37 °C for 30 min prior to incubation with keratin azure. Control reactions received solvent. Control reactions received an equivalent volume of the corresponding solvent. Keratinolytic activity was subsequently assessed using the keratin azure assay described in Section 2.3 by measuring the solubilized peptide content.

2.7. Determination of Enzyme Deactivation Constant

The thermal stability of the enzymes was evaluated by determining the first-order deactivation constant (k_d) [31,32] based on residual activity measurements over time. The assumption of first-order deactivation kinetics was validated by fitting the experimental residual activity data to an exponential decay model. A linear relationship was observed when plotting $\ln(A_t/A_0)$ versus time, and the corresponding regression analyses yielded high coefficients of determination (R^2), indicating good agreement with first-order kinetics. Similar first-order deactivation behavior has been widely reported for plant-derived proteases under thermal stress conditions. Enzyme samples were incubated at defined temperatures (37 °C and 50 °C), and residual enzymatic activity was measured at predetermined time points up to 48 h. The relative activity (A_t) at each time point was expressed as a percentage of the initial activity (A_0), which was set to 100%.

Assuming first-order deactivation kinetics, the loss of enzymatic activity over time was described by the following equation [33]:

$$A_t = A_0 \exp(-k_d t)$$

where A_t is the residual activity at time t(h), A_0 is the initial activity, and k_d is the deactivation rate constant (h^{-1}). The k_d values were obtained by nonlinear regression analysis of the relative activity data using an exponential decay model. Curve fitting was performed

using statistical software, and the goodness of fit was evaluated based on the coefficient of determination (R^2). All experiments were conducted at least in triplicate, and k_d values are reported as mean ± standard deviation.

Lower k_d values indicate greater enzymatic stability and slower loss of activity under the tested conditions.

2.8. In Vitro Evaluation of Cytotoxicity and Functional Effect

RAW 264.7 cells (KCLB, Seoul, Republic of Korea) were cultured in DMEM (Hyclone, Logan, UT, USA) supplemented with 10% FBS (Thermo Fisher Scientific, Waltham, MA, USA) and 1% penicillin/streptomycin (Thermo Fisher Scientific, Waltham, MA, USA). Cells were seeded at 2×10^5 cells/well in 24-well plates (SPL Life Sciences Co., Ltd., Pocheon, Republic of Korea) and incubated at 37 °C with 5% CO_2 humidified atmosphere for 24 h. Cells were then treated with 1 μg/mL lipopolysaccharide (LPS; Sigma-Aldrich, St. Louis, MO, USA), with or without BM-derived enzyme (0.125–8%), for 24 h. The total culture volume in each well was 1 mL. After 24 h of treatment, culture supernatants were collected by gentle centrifugation and used for nitric oxide (NO) measurement, representing extracellular NO released by RAW 264.7 cells. The remaining adherent cells were subsequently subjected to cell viability analysis.

NO production [34] was measured using the NO Plus Detection Kit (iNtRON Biotechnology, Seongnam, Republic of Korea). Supernatants (100 μL) were mixed with equal volumes of N1 and N2 buffers and incubated for 10 min at room temperature. Absorbance was measured at 540 nm, and a standard curve was constructed using sodium nitrite. A linear calibration curve was obtained over the concentration range of 0–250 μM. Based on the calibration data ($y = 0.0092x + 0.0594$, $R^2 = 0.9988$), the LOD and LOQ were calculated as 0.21 μM and 0.63 μM, respectively.

For cell viability, 100 μL of EZ-Cytox reagent (DoGenBio Co., Ltd., Seoul, Republic of Korea) was added to each well and the cells were incubated for 1 h at 37 °C. Absorbance was measured at 450 nm.

Elastase inhibition was determined using porcine pancreatic elastase and N-succinyl-Ala-Ala-Ala-p-nitroanilide (SANA; Sigma-Aldrich, St. Louis, MO, USA). Reaction mixtures contained 40 μL sample solution, 40 μL elastase (0.4 U/mg; Sigma-Aldrich, St. Louis, MO, USA), and 200 μL of 1 mM SANA in Tris-HCl (pH 8.0). After incubation at 25 °C for 5 min, absorbance was read at 405 nm. The calibration curve showed good linearity ($y = 5.0068x + 2.0106$, $R^2 = 0.9908$), and the calculated LOD and LOQ values were 0.014 μg/mL and 0.043 μg/mL, respectively.

2.9. In-Use Clinical Evaluation of BM-Derived Keratinase Formulation

An in-use test was conducted at the Korea Dermatology Research Institute (KDRI), a certified dermatological research institution affiliated with GFC Life science. Ltd. (Hwaseong-si, Gyeonggi-do, Republic of Korea). The study was approved by the Institutional Review Board (IRB No. KDRI-IRB-250198).

Eleven healthy adults (aged 49–55 years; Table 1) participated in a 4-week trial to assess the efficacy and safety of a 0.5% BM-derived keratinase solution, prepared by dissolving the freeze-dried enzyme powder in sterile triple-distilled water (TDW) without additional active ingredients. Participants applied 1 mL of the solution evenly to a designated facial area—defined by the intersection of a horizontal line from the nasal ala and the mid-pupillary line—twice daily after cleansing. Participants were asked not to change their daily skin care routine other than the application of the test product. Usage was self-recorded in a provided diary. This instruction was intended to minimize the potential confounding effects of other cosmetic products on the study outcomes.

Table 1. Basic demographic information of study subjects. Summary of demographic characteristics of the participants enrolled in the clinical trial, including age and gender.

No	ID *	Age	Gender
1	2539	49	Female
2	6895	51	Female
3	2513	52	Female
4	3169	53	Female
5	4434	53	Female
6	6528	53	Female
7	1169	55	Female
8	3145	55	Female
9	2301	58	Female
10	6834	58	Female
11	1304	59	Female

* Participant IDs correspond to unique identification numbers assigned by the Korean Dermatology Research Institute (KDRI).

The study was designed as a single-arm, in-use evaluation, and efficacy was assessed by within-subject comparison to baseline values to minimize inter-individual variability. All measurements were performed under standardized conditions in a climate-controlled room maintained at 22 ± 2 °C and 45 ± 5% relative humidity, following a 30 min acclimatization period, in accordance with the manufacturers' recommended protocols for dermatological instrumental measurements.

Scaly skin improvement was evaluated by corneocyte collection using the Corneofix D100 (Courage + Khazaka electronic GmbH, Köln, Germany), followed by image analysis with the Visioscan® VC20 Plus (Courage + Khazaka electronic GmbH, Köln, Germany). Skin surface characteristics, including smoothness (SEsm), were quantitatively assessed using the same device. Stratum corneum hydration was measured with a Corneometer® CM825 (Courage + Khazaka electronic GmbH, Köln, Germany), and deeper moisture content was further assessed using the MoistureMeter EpiD® (Delfin Technologies Ltd., Kuopio, Finland). Dermatological evaluations [35] were conducted at baseline, after 2 weeks, and after 4 weeks to monitor signs of cutaneous irritation or adverse effects. All measurements were taken under standardized conditions after 30 min of acclimatization.

2.10. Statistical Analysis

Statistical analyses were performed using IBM SPSS Statistics v.28.0 (IBM Corp., Armonk, NY, USA). Data normality was assessed using the Shapiro–Wilk test [36]. For normally distributed data, paired *t*-tests were used for comparisons of pre- and post-treatment values [37], and repeated measures ANOVA was applied for datasets with multiple time points. Statistical significance was defined as $p < 0.05$. Principal component analysis (PCA) [38] was performed and visualized using the ggplot2 package in R (version 4.4.3).

3. Results and Discussion

3.1. Protein Yield and Keratinolytic Activity of BM-Derived Enzyme

Crude extracts were prepared from bitter melon (BM), papaya (CP), and date palm (PD) using the same extraction procedure to comparatively evaluate protein yield and keratinolytic activity. Among the three, the BM extract exhibited the highest protein concentration (1.44 mg/mL ± 0.04) (Figure 1A), indicating efficient protein recovery. Correspondingly, the BM-derived enzyme induced the greatest increase in absorbance at 595 nm (0.89 ± 0.06), reflecting superior keratin degradation activity relative to CP (0.80 ± 0.08) and PD (0.34 ± 0.07) (Figure 1B).

These results demonstrate that the BM-derived enzyme possesses stronger keratinolytic activity under the tested conditions. Given their comparable protein yields, BM- and CP-derived keratinolytic activities were further compared in detail.

3.2. Effects of Temperature and pH on Keratinolytic Stability

To evaluate the thermal and pH stability of the plant-derived keratinases under conditions relevant to cosmetic formulation and storage, enzyme solutions were incubated at various temperatures and pH levels for five days, followed by measurement of residual keratinolytic activity. The BM-derived enzyme retained over 80% of its activity even after prolonged incubation at 70 °C, whereas papain exhibited maximal activity at 37 °C but rapidly lost its function above 50 °C [11,39,40], becoming nearly inactive at 70 °C (Figure 1C). In terms of pH stability, the BM-derived enzyme maintained over 75% of its peak activity within the pH range of 5.0–9.0, while papain demonstrated stability primarily between pH 6.5 and 8.0 (Figure 1D). These results underscore the greater robustness of the BM-derived enzyme under thermal and pH stress, supporting its suitability for cosmetic applications requiring formulation and storage stability.

To further support these findings, we conducted a short-term thermal activation test in which enzymes were exposed to different temperatures (45 °C and 70 °C) for 1 h. While papain showed only a modest decrease in activity at 45 °C and a marked loss at 70 °C, the BM-derived enzyme exhibited its highest relative activity after a 1 h incubation at 70 °C, suggesting heat-induced activation rather than denaturation (Figure 1F). This unique property was consistent with previous findings on aspartic proteases isolated from bitter melon, which also demonstrated increased activity upon heating [25]. Taken together, these results highlight the distinctive thermodynamic characteristics of the BM-derived enzyme and its potential as a heat-stable, multifunctional bioactive component in cosmetic formulations.

3.3. Influence of Protease Inhibitors on Keratinolytic Activity

To determine the protease class responsible for keratinolytic activity, inhibition assays were conducted using specific protease inhibitors: Pepstatin A (aspartic protease inhibitor), E-64 (cysteine protease inhibitor), and EDTA (metalloprotease inhibitor). The enzymatic activities of the BM-derived enzyme and papain (Sigma-Aldrich, USA) were compared under identical conditions.

Without inhibitors, enzymatic activity was normalized to 100%. Treatment with Pepstatin A (1 μM) significantly suppressed the relative activity of BM-derived enzyme to 30.7% ± 9.2 (mean ± SD, $n = 3$), indicating approximately 69.3% inhibition compared to control ($p = 0.0002$, Student's t-test) (Figure 1E). This marked inhibition supports that the BM-derived keratinolytic enzyme predominantly functions as an aspartic protease. Conversely, papain activity was unaffected by Pepstatin A (100.6% ± 5.8), consistent with its classification as a cysteine protease.

E-64 treatment (1 μM) reduced the relative activity of papain to 22.9% ± 8.9, whereas BM-derived enzyme activity decreased slightly to 97.2% ± 4.3 (Figure 1E). EDTA (10 μM) caused partial inhibition of both enzymes (BM: 91.2% ± 4.3; papain: 83.9% ± 6.0), indicating a possible role of metal ions in maintaining enzyme structure or catalytic activity.

Overall, these results indicate that the BM-derived enzyme is predominantly an aspartic protease, in contrast to papain, a cysteine protease. Aspartic proteases are a well-characterized class of proteolytic enzymes, possessing conserved catalytic aspartate residues and typically exhibiting optimal activity under acidic to neutral conditions [41,42]; moreover, they are specifically inhibited by pepstatin A, consistent with the inhibitor profile observed in the present study. This classification aligns with current knowledge on

plant aspartic proteases and supports the functional distinction between the BM-derived keratinase and papain.

3.4. Enhanced Thermal Stability of BM-Derived Keratinase Revealed by Deactivation Kinetics

The thermal deactivation behavior of the BM-derived keratinase was quantitatively evaluated and compared with that of CP-derived keratinase by assuming first-order deactivation kinetics. The time-dependent decrease in relative enzymatic activity at 37 °C and 50 °C was fitted to the first-order kinetic model [33], and the corresponding deactivation constants (k_d) were calculated from the linear regression of $\ln(A_t/A_0)$ versus time.

At 37 °C, both enzymes exhibited relatively low deactivation rates, indicating good stability under near-physiological conditions (Figure 2). The k_d value of the BM-derived enzyme was 0.00165 ± 0.00012 h^{-1}, while that of papain was slightly lower at 0.00089 ± 0.00013 h^{-1}. These results indicate that both enzymes maintained high catalytic activity over 48 h at 37 °C, with only minor activity loss.

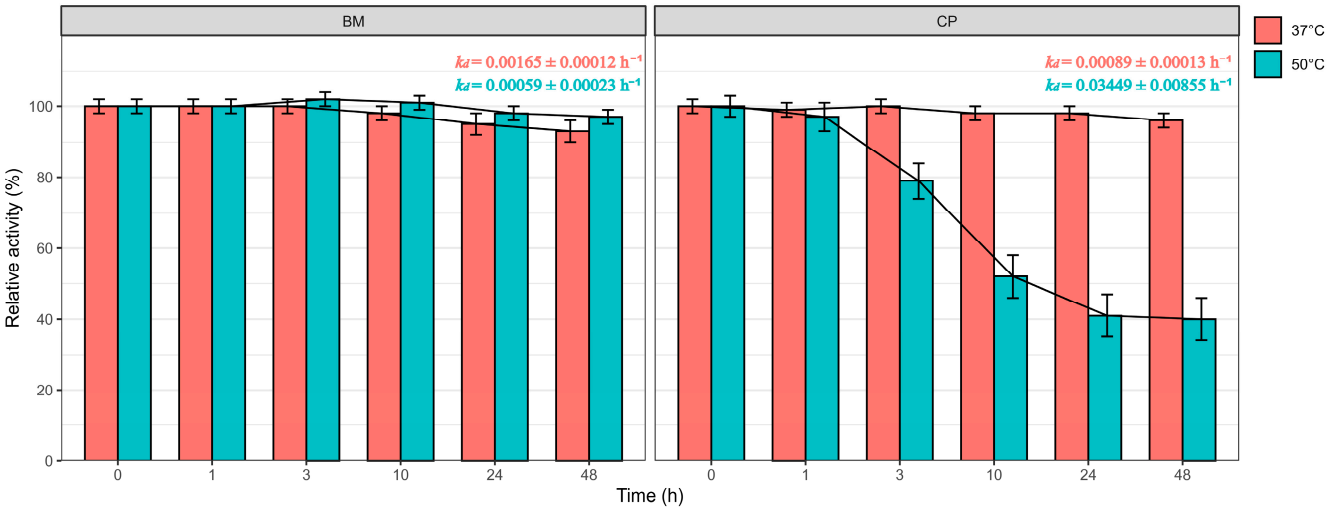


Figure 2. Comparison of deactivation constants (k_d) of BM-derived and CP-derived keratinases at 37 °C and 50 °C. Deactivation constants were determined by fitting residual enzyme activity data to a first-order deactivation model. Data are presented as mean ± SD.

In contrast, marked differences in thermal stability were observed at 50 °C. The BM-derived keratinase retained high activity throughout the incubation period, yielding a low k_d value of 0.00059 ± 0.00023 h^{-1}. In comparison, papain underwent rapid thermal deactivation, with a k_d value of 0.03449 ± 0.00855 h^{-1}, approximately 58-fold higher than that of the BM-derived enzyme at the same temperature (Figure 2). This pronounced increase in k_d for papain reflects a substantial loss of enzymatic activity under elevated temperature conditions.

Overall, these results demonstrate that the BM-derived keratinase exhibits significantly enhanced thermal stability compared with papain, particularly at elevated temperatures relevant to cosmetic formulation processing and storage. The low deactivation constants observed for the BM enzyme support its suitability as a robust and thermostable protease for cosmetic applications.

3.5. In Vitro Cytotoxicity and Functional Effects

The cytotoxic potential of the BM-derived enzyme was first evaluated in RAW 264.7 macrophage cells over a broad concentration range (0.125–8%). Cell viability remained above 95% at all tested concentrations, with no statistically significant differences compared to the untreated control (Figure 3A). These findings indicate that the BM-derived

enzyme does not exert detectable cytotoxic effects under the experimental conditions, supporting its suitability for further functional evaluation and potential topical use.

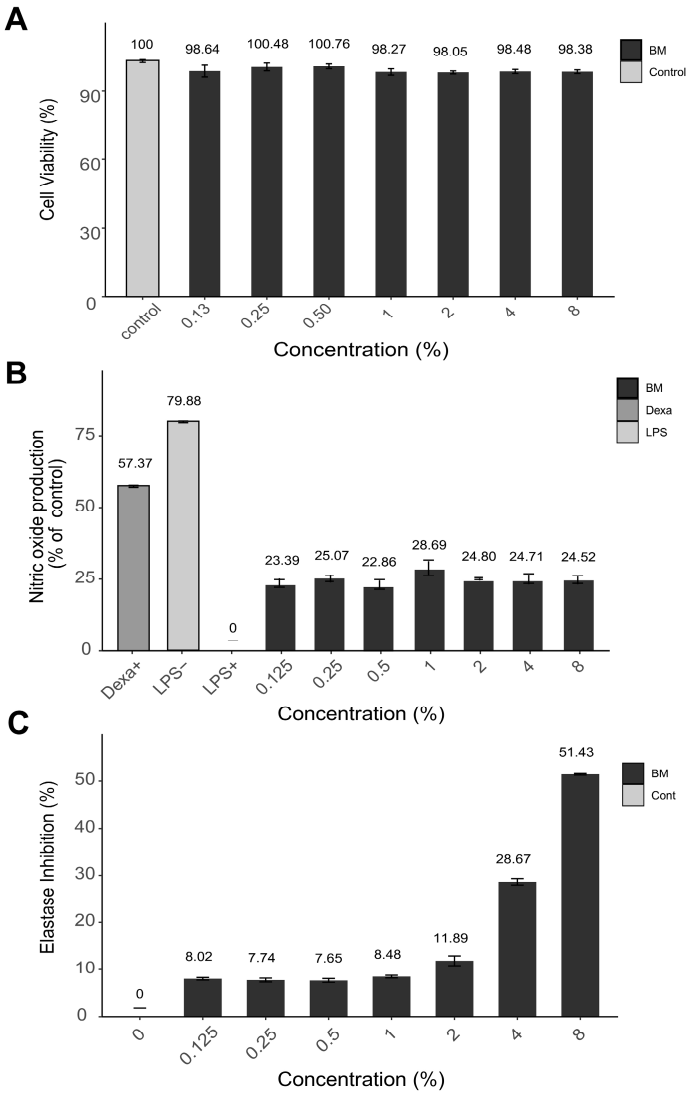


Figure 3. In vitro efficacy of BM-derived enzyme in (**A**) cell viability, (**B**) nitric oxide inhibition in LPS-stimulated macrophages, and (**C**) elastase inhibition. All data are presented as mean ± standard deviation from three independent experiment.

The anti-inflammatory activity of the enzyme was subsequently assessed by measuring nitric oxide (NO) production in lipopolysaccharide (LPS)-stimulated RAW 264.7 cells. Treatment with the BM-derived enzyme resulted in a significant reduction in NO levels, with inhibition ranging from 22.9% to 28.7% across the tested concentrations (Figure 3B). Although a strict dose-dependent trend was not observed, the consistent suppression of NO production suggests that the enzyme exerts a stable anti-inflammatory effect over a wide concentration range.

Elastase inhibitory activity was also examined to explore potential anti-aging functionality. In contrast to the NO inhibition results, elastase inhibition increased progressively with enzyme concentration, demonstrating a clear dose-dependent response (Figure 3C). The highest concentration (8%) achieved 51.4% ± 0.16 inhibition, indicating a substantial capacity to interfere with elastase-mediated degradation of extracellular matrix components. Together, these results indicate that the BM-derived enzyme exhibits low cytotoxicity alongside anti-inflammatory and elastase-inhibitory activities in vitro.

3.6. In-Use Clinical Efficacy of BM-Derived Keratinase Formulation

A 4-week clinical trial involving topical application of the BM-derived keratinase formulation demonstrated statistically significant improvements in multiple skin parameters (Figure 4 and Table 2). Principal component analysis (PCA) of efficacy data revealed clear separation between baseline and week 4, with the first two components accounting for 78.4% of variance (Figure 4A). Vectors for desquamation, skin surface smoothness (SEsm), and moisture content shifted consistently toward the week 4 cluster, indicating a coordinated multidimensional improvement in skin condition.

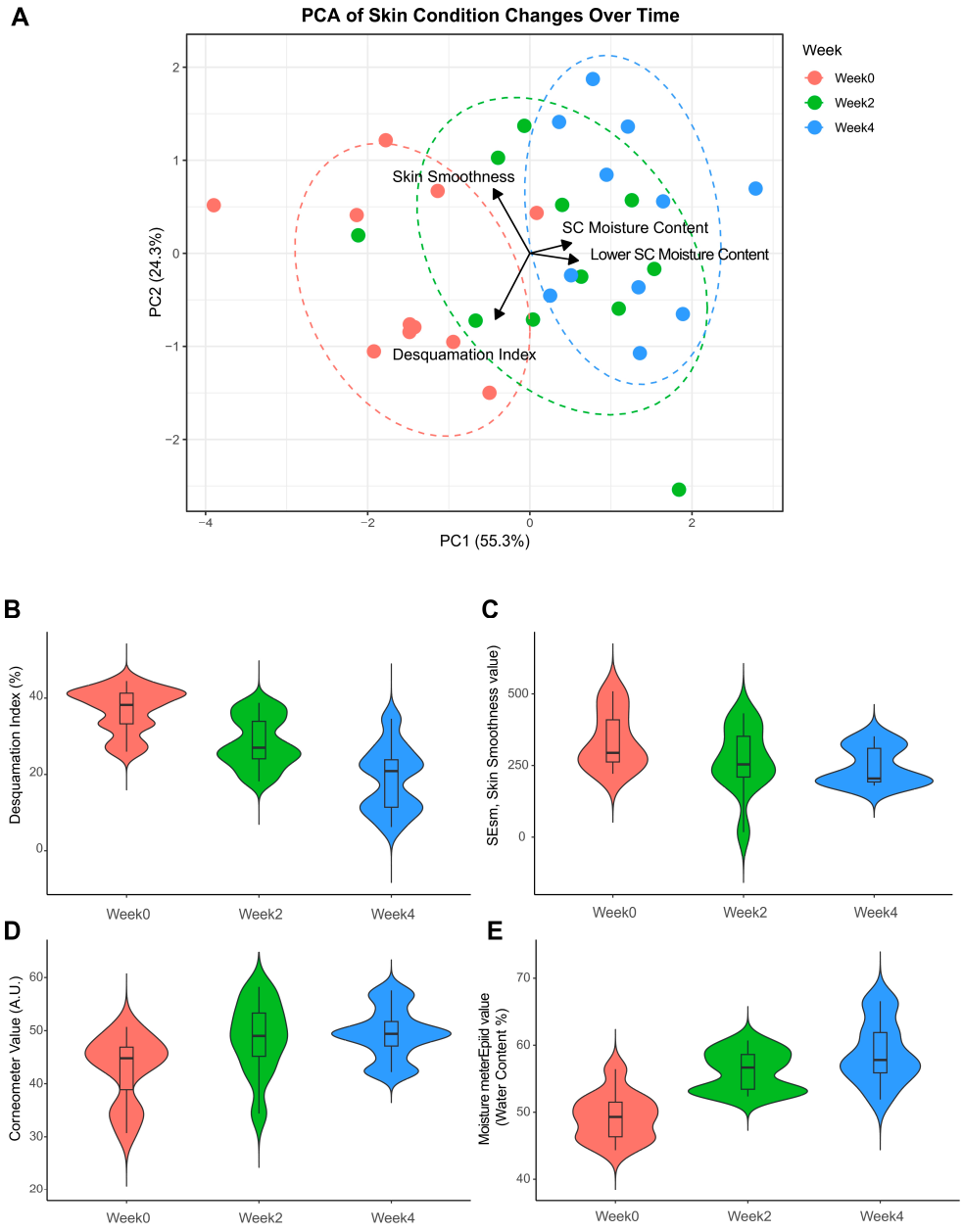


Figure 4. Clinical efficacy of the BM-derived keratinase formulation over a 4-week period. (**A**) Principal component analysis (PCA) of all skin parameters across time points. Vectors indicate the direction and magnitude of contribution for each parameter, demonstrating an overall shift in skin condition following treatment. (**B**–**E**) Violin plots showing changes in (**B**) desquamation index, (**C**) skin surface smoothness (SEsm), (**D**) stratum corneum hydration, and (**E**) water content in the lower SC layer ($p < 0.001$). Data are presented as mean ± standard deviation, overlaid with distributions of individual values.

Table 2. Clinical evaluation of improvements following a 4-week in-use test of keratinase solution derived from bitter melon.

	Week	Mean ± S.D. *	Improvement Rate (%)	*p*-Value
Desquamation Index	Week 0	36.95 ± 5.98	-	<0.001
	Week 2	28.37 ± 6.75	23.73	
	Week 4	18.80 ± 8.75	49.88	
Skin Smoothness Value (SEsm, A.U.)	Week 0	337.61 ± 101.11	-	<0.001
	Week 2	279.72 ± 79.70	16.40	
	Week 4	246.61 ± 66.27	26.04	
Moisture Content of SC (Corneometer Value, A.U.)	Week 0	42.77 ± 6.47	-	<0.001
	Week 2	47.76 ± 6.21	12.16	
	Week 4	49.47 ± 4.90	16.88	
Moisture Content in the Lower Layer of SC (Water content %)	Week 0	49.32 ± 3.55	-	<0.001
	Week 2	56.03 ± 3.03	13.93	
	Week 4	58.90 ± 4.72	19.70	

* Averages that do not share characters have a statistically significant difference ($p < 0.05$). By Bonferroni method.

Quantitative analysis confirmed marked improvements over the treatment period (Table 2). The desquamation index was reduced by 49.88%, decreasing from 36.95 ± 5.98 at baseline to 18.80 ± 8.75 at week 4 ($p < 0.001$) (Figure 4B). Skin surface smoothness also improved significantly, with SEsm values decreasing by 26.04% from 337.61 ± 101.11 to 246.61 ± 66.27 ($p < 0.001$) (Figure 4C). Stratum corneum hydration, assessed by Corneometer measurements, increased by 16.88% (42.77 ± 6.47 to 49.47 ± 4.90; $p < 0.001$) (Figure 4D), while water content in the lower SC layers increased by 19.70% (49.32 ± 3.55 to 58.90 ± 4.72; $p < 0.001$) (Figure 4E). These results demonstrate that BM-derived keratinase not only improves exfoliation and surface texture but also enhances hydration, supporting its potential as a multifunctional cosmetic bioactive.

Representative Visioscan® images demonstrated a visible reduction in surface scaliness after four weeks of treatment (Figure 5A); while corresponding three-dimensional skin surface images revealed a smoother and more uniform skin texture (Figure 5B), further supporting the quantitative findings. No adverse reactions or signs of irritation were reported by any of the 11 participants throughout the study, confirming the formulation's safety and tolerability under the tested conditions.

Clinical evidence supporting the efficacy of enzyme-based exfoliants remains relatively limited compared to chemical exfoliants such as AHAs and BHAs [10,43]. Previous studies on enzymatic exfoliation have mainly focused on short-term effects or in vitro models [9]. The present in-use clinical study provides human evidence that a plant-derived keratinase can simultaneously improve desquamation, skin texture, and hydration without irritation.

Although participants were instructed to refrain from introducing new cosmetic products or functional ingredients during the study period, individual skincare routines were not fully standardized. The specific compositions and potential interactions of participants' habitual skincare products were therefore not systematically evaluated. While a within-group comparison design was employed to minimize inter-individual variability, the influence of personal skincare routines cannot be completely excluded and should be considered a limitation of this study. In addition, as this investigation was designed as a pilot in-use clinical evaluation with a relatively limited sample size, the results should be interpreted with caution. Future large-scale, controlled clinical studies employing stricter control of skincare regimens or wash-out periods are warranted to further substantiate and clarify the independent efficacy of the BM-derived keratinase formulation.

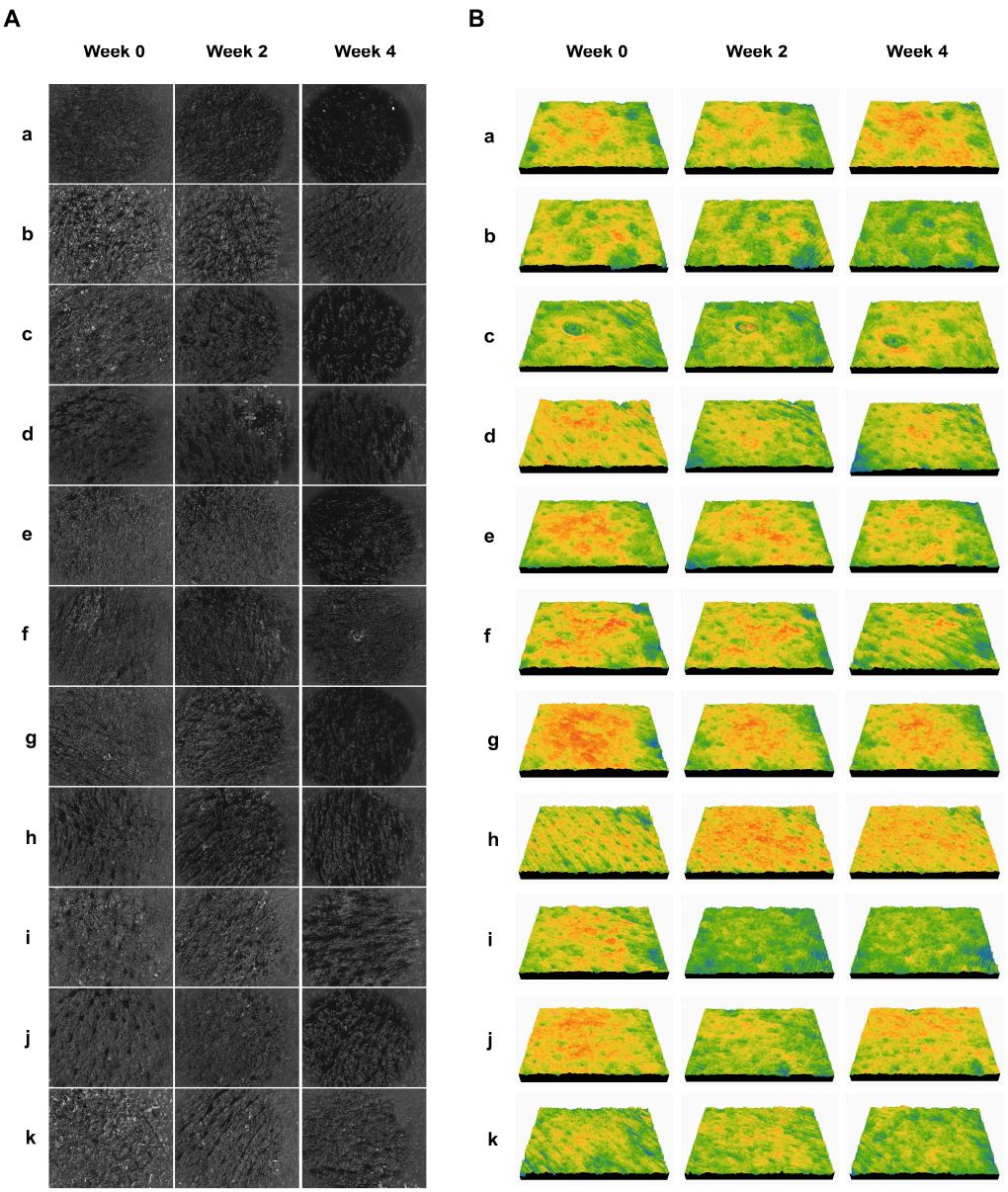


Figure 5. Representative skin surface topography (**A**) and 3D skin surface images (**B**) captured using Visioscan® VC 98 before and after 4-week application of the BM-derived keratinase formulation. Panels (**a**–**k**) represent individual participants. Within each row, images from left to right correspond to: (week 0) baseline (pre-treatment), (week 2) after 2 weeks of treatment, and (week 4) after 4 weeks of treatment.

4. Conclusions

This study addresses key limitations associated with conventional plant-derived cosmetic enzymes—particularly their insufficient thermal and formulation stability—by demonstrating the feasibility of a keratinolytic enzyme derived from *Momordica charantia* as a robust and effective cosmetic ingredient. The BM-derived keratinase exhibited strong keratin-degrading activity while maintaining high stability under elevated temperature and diverse pH conditions, overcoming a major constraint that restricts the practical use of many natural proteases in cosmetic formulations.

Beyond its physicochemical robustness, the enzyme retained the intrinsic biological advantages associated with bitter melon, a food-grade plant traditionally recognized for its skin-beneficial properties. In vitro analyses confirmed that the BM-derived keratinase combines low cytotoxicity with anti-inflammatory and elastase-inhibitory activities, sug-

gesting that its exfoliating action may be accompanied by additional skin-conditioning and protective effects. Importantly, these multifunctional properties were substantiated in a four-week in-use clinical study, which demonstrated significant improvements in desquamation, skin surface smoothness, and hydration without inducing irritation.

Collectively, these findings propose the Bitter melon–derived keratinase as a naturally sourced, multifunctional cosmetic bioactive that enables effective yet mild enzymatic exfoliation while providing ancillary skin benefits. By integrating the traditional efficacy of bitter melon with enhanced enzymatic stability, this work presents a viable strategy for expanding the use of natural plant enzymes in cosmetic formulations and offers a promising alternative to commonly used proteases such as papain.

Author Contributions: S.P.: Conceptualization, formal analysis, visualization, writing, reviewing, and project administration. J.E.L.: Investigation and formal analysis. J.W.M.: Conceptualization, reviewing, and supervision. H.C.K.: Supervision. All authors have read and agreed to the published version of the manuscript.

Funding: This study was supported by GFC Life Science Co., Ltd., Republic of Korea. We would like to thank Suhyun Lee, Eunji Eom, and Dong-Hwan Lee from the Korea Institute of Dermatological Sciences for their support in the clinical evaluation. This research received no external funding.

Institutional Review Board Statement: The study was conducted in accordance with the Declaration of Helsinki and approved by the Institutional Review Board of the Korea Dermatology Research Institute (KDRI) (IRB No. KDRI-IRB-250198, KDRI-IRB-250199, KDRI-IRB-25200; study protocol approved on 12 February 2025, study results approved on 26 March 2025).

Informed Consent Statement: Informed consent was obtained from all subjects involved in the study.

Data Availability Statement: All relevant data is provided within the manuscript.

Conflicts of Interest: All authors are employees of GFC Life Science Co., Ltd. The funders had role in the design of the study; in the collection, analyses or interpretation of data; in the writing of the manuscript; or in the decision to publish the results.

References

1. Akiyama, F.; Takahashi, N.; Ueda, Y.; Tada, S.; Takeuchi, N.; Ohno, Y.; Kihara, A. Correlations between skin condition parameters and ceramide profiles in the stratum corneum of healthy individuals. *Int. J. Mol. Sci.* **2024**, *25*, 8291. [CrossRef] [PubMed]
2. Behalpade, S.; Gajbhiye, S.; Hills, S. Review Article: Skin Care With Exfoliation Process. *Int. J. Corrent Sci.* **2022**, *12*, 372–379.
3. Knaggs, H.; Lephart, E.D. Enhancing skin anti-aging through healthy lifestyle factors. *Cosmetics* **2023**, *10*, 142. [CrossRef]
4. Green, B.A.; Van Scott, E.J.; Yu, R.J. Clinical uses of hydroxyacids. In *Cosmetic Dermatology: Products and Procedures*; John Wiley & Sons Ltd.: Hoboken, NJ, USA, 2022; pp. 430–441.
5. Smith, W.P.; Bishop, M.A.; Norton, S.J. Cosmetic benefits derived from the topical application of acid proteases. In *Skin Moisturization*; CRC Press: Boca Raton, FL, USA, 2016; pp. 419–432.
6. Tören, E.; Mazari, A.A.; Buzgo, M. Exploring the efficacy of AHA–BHA infused nanofiber skin masks as a topical treatment for acne vulgaris. *J. Appl. Polym. Sci.* **2024**, *141*, e55203. [CrossRef]
7. Hwang, J.-h.; Lee, S.; Lee, H.G.; Choi, D.; Lim, K.-M. Evaluation of skin irritation of acids commonly used in cleaners in 3D-reconstructed human epidermis model, KeraSkin™. *Toxics* **2022**, *10*, 558. [CrossRef]
8. Soleymani, T.; Lanoue, J.; Rahman, Z. A practical approach to chemical peels: A review of fundamentals and step-by-step algorithmic protocol for treatment. *J. Clin. Aesthet. Dermatol.* **2018**, *11*, 21.
9. Venetikidou, M.; Lykartsi, E.; Adamantidi, T.; Prokopiou, V.; Ofrydopoulou, A.; Letsiou, S.; Tsoupras, A. Proteolytic Enzyme Activities of Bromelain, Ficin, and Papain from Fruit By-Products and Potential Applications in Sustainable and Functional Cosmetics for Skincare. *Appl. Sci.* **2025**, *15*, 2637. [CrossRef]
10. Trevisol, T.C.; Henriques, R.O.; Souza, A.J.A.; Furigo, A., Jr. An overview of the use of proteolytic enzymes as exfoliating agents. *J. Cosmet. Dermatol.* **2022**, *21*, 3300–3307. [CrossRef]
11. Trevisol, T.C.; Henriques, R.O.; Cesca, K.; Souza, A.J.A.; Furigo, A., Jr. In vitro effect on the proteolytic activity of papain with proteins of the skin as substrate. *Int. J. Cosmet. Sci.* **2022**, *44*, 542–554. [CrossRef]

12. Sujitha, P.; Shanthi, C. Importance of enzyme specificity and stability for the application of proteases in greener industrial processing—A review. *J. Clean. Prod.* **2023**, *425*, 138915. [CrossRef]
13. Chavan, M. Biological skin exfoliation based on optimized and stabilized papain enzyme: PO10. *Int. J. Cosmet. Sci.* **2015**, *37*, 153–154.
14. Pinto, C.A.S.d.O.; Lopes, P.S.; Sarruf, F.D.; Polakiewicz, B.; Kaneko, T.M.; Baby, A.R.; Velasco, M.V.R. Comparative study of the stability of free and modified papain incorporated in topical formulations. *Braz. J. Pharm. Sci.* **2011**, *47*, 751–760. [CrossRef]
15. Ahmad, N.; Hasan, N.; Ahmad, Z.; Zishan, M.; Zohrameena, S. *Momordica charantia*: For traditional uses and pharmacological actions. *J. Drug Deliv. Ther.* **2016**, *6*, 40–44. [CrossRef]
16. Kumar, K.S.; Bhowmik, D. Traditional medicinal uses and therapeutic benefits of *Momordica charantia* Linn. *Int. J. Pharm. Sci. Rev. Res.* **2010**, *4*, 23–28.
17. Fang, E.F.; Ng, T.B. Bitter gourd (*Momordica charantia*) is a cornucopia of health: A review of its credited antidiabetic, anti-HIV, and antitumor properties. *Curr. Mol. Med.* **2011**, *11*, 417–436. [CrossRef]
18. Gupta, M.; Sharma, S.; Gautam, A.K.; Bhadauria, R. *Momordica charantia* Linn. (Karela): Nature's silent healer. *Int. J. Pharm. Sci. Rev. Res.* **2011**, *11*, 32–37.
19. Singh, J.; Cumming, E.; Manoharan, G.; Kalasz, H.; Adeghate, E. Medicinal chemistry of the anti-diabetic effects of *Momordica charantia*: Active constituents and modes of actions. *Open Med. Chem. J.* **2011**, *5*, 70. [CrossRef]
20. Grover, J.K.; Yadav, S.P. Pharmacological actions and potential uses of *Momordica charantia*: A review. *J. Ethnopharmacol.* **2004**, *93*, 123–132. [CrossRef]
21. Nerurkar, P.V.; Lee, Y.-K.; Nerurkar, V.R. *Momordica charantia* (bitter melon) inhibits primary human adipocyte differentiation by modulating adipogenic genes. *BMC Complement. Altern. Med.* **2010**, *10*, 34. [CrossRef]
22. Joseph, B.; Jini, D. Antidiabetic effects of *Momordica charantia* (bitter melon) and its medicinal potency. *Asian Pac. J. Trop. Med.* **2013**, *3*, 93–102. [CrossRef]
23. Kim, H.-W.; Shin, H.; Hwang, D.; Lee, J.; Jeong, H.; Kim, D. Functional cosmetic characteristics of *Momordica charantia* fruit extract. *Korean Chem. Eng. Res.* **2015**, *53*, 289–294. [CrossRef]
24. Sagástegui-Guarniz, W.A.; Silva-Correa, C.R.; Villarreal-La Torre, V.E.; González-Blas, M.V.; Sagástegui-Guarniz, W.O.; Calderón-Peña, A.A.; Aspajo-Villalaz, C.L.; Cruzado-Razco, J.L.; Hilario-Vargas, J. Wound healing by topical application of *Momordica charantia* L. formulations on mice. *Vet. World* **2021**, *14*, 2699–2704. [CrossRef] [PubMed]
25. Wang, L.; Wang, M.; Li, Q.; Cai, T.; Jiang, W. Partial properties of an aspartic protease in bitter gourd (*Momordica charantia* L.) fruit and its activation by heating. *Food Chem.* **2008**, *108*, 496–502. [CrossRef] [PubMed]
26. Jena, R.; Ranade, D.; Chaudhari, P.; Salunke, A.; Mahamuni, A.; Gairola, S. Systematic Development and Validation of a Bradford-Based Protein Quantification Method for Novel Multi-Dose R21 Malaria Vaccine Formulated with 2-Phenoxy Ethanol (2-PE). *Vaccines* **2025**, *14*, 25. [CrossRef]
27. Yong, J.; Hakobyan, K.; Xu, J.; Mellick, A.S.; Whitelock, J.; Liang, K. Comparison of protein quantification methods for protein encapsulation with ZIF-8 metal-organic frameworks. *Biotechnol. J.* **2023**, *18*, 2300015. [CrossRef]
28. Yoshida, H.; Okamoto, K.; Iwamoto, T.; Sakai, E.; Kanaoka, K.; Hu, J.-P.; Shibata, M.; Hotokezaka, H.; Nishishita, K.; Mizuno, A. Pepstatin A, an aspartic proteinase inhibitor, suppresses RANKL-induced osteoclast differentiation. *J. Biochem.* **2006**, *139*, 583–590. [CrossRef]
29. Baruwa, A.O.; Martins, J.N.; Maravic, T.; Mazzitelli, C.; Mazzoni, A.; Ginjeira, A. Effect of endodontic irrigating solutions on radicular dentine structure and matrix metalloproteinases—A comprehensive Review. *Dent. J.* **2022**, *10*, 219. [CrossRef]
30. Schepetkin, I.A.; Fischer, A.M. Activity-Based Profiling of Papain-like Cysteine Proteases During Late-Stage Leaf Senescence in Barley. *Plants* **2025**, *14*, 3132. [CrossRef]
31. Wojcik, M.; Miłek, J. A new method to determine optimum temperature and activation energies for enzymatic reactions. *Bioproc. Biosyst. Eng.* **2016**, *39*, 1319–1323. [CrossRef]
32. Bhunia, B.; Basak, B.; Mandal, T.; Bhattacharya, P.; Dey, A. Effect of pH and temperature on stability and kinetics of novel extracellular serine alkaline protease (70 kDa). *Int. J. Biol. Macromol.* **2013**, *54*, 1–8. [CrossRef]
33. Sadana, A. *Biocatalysis: Fundamentals of Enzyme Deactivation Kinetics*; Prentice Hall: Englewood Cliffs, NJ, USA, 1991.
34. Facchin, B.M.; Dos Reis, G.O.; Vieira, G.N.; Mohr, E.T.B.; da Rosa, J.S.; Kretzer, I.F.; Demarchi, I.G.; Dalmarco, E.M. Inflammatory biomarkers on an LPS-induced RAW 264.7 cell model: A systematic review and meta-analysis. *Inflamm. Res.* **2022**, *71*, 741–758. [CrossRef] [PubMed]
35. Müller, R.; Lienau, C. Three-dimensional analysis of light propagation through uncoated near-field fibre probes. *J. Microsc.* **2001**, *202*, 339–346. [CrossRef] [PubMed]
36. Shapiro, S.S.; Wilk, M.B. An analysis of variance test for normality (complete samples). *Biometrika* **1965**, *52*, 591–611. [CrossRef]
37. Altman, D.G. *Practical Statistics for Medical Research*; Chapman and Hall/CRC: New York, NY, USA, 1990.
38. Jolliffe, I.T.; Cadima, J. Principal component analysis: A review and recent developments. *Philos. Trans. R. Soc. A Math. Phys. Eng. Sci.* **2016**, *374*, 20150202. [CrossRef]

39. Yang, H.R.; Zahan, M.N.; Yoon, Y.; Kim, K.; Hwang, D.H.; Kim, W.H.; Rho, I.R.; Kim, E.; Kang, C. Unveiling the potent fibrino(geno)lytic, anticoagulant, and antithrombotic effects of papain, a cysteine protease from *Carica papaya* latex using κ-carrageenan rat tail thrombosis model. *Int. J. Mol. Sci.* **2023**, *24*, 16770. [CrossRef]
40. Qadeer, A.; Zaman, M.; Khan, R. Inhibitory effect of post-micellar SDS concentration on thermal aggregation and activity of papain. *Biochemistry* **2014**, *79*, 785–796. [CrossRef]
41. Wei, M.; Chen, P.; Zheng, P.; Tao, X.; Yu, X.; Wu, D. Purification and characterization of aspartic protease from Aspergillus niger and its efficient hydrolysis applications in soy protein degradation. *Microb. Cell Factories* **2023**, *22*, 42. [CrossRef]
42. Figueiredo, L.; Santos, R.B.; Figueiredo, A. Defense and offense strategies: The role of aspartic proteases in plant–pathogen interactions. *Biology* **2021**, *10*, 75. [CrossRef]
43. Zhou, H.; Tang, L.; Zhang, W.; Li, X.; Li, R.; Dong, C. Development and Clinical Evaluation of a Supramolecular Acid-Enzyme Complex for Skin Exfoliation, Sebum Control, and Pore Refinement. *J. Dermatol. Sci. Cosmet. Technol.* **2025**, *2*, 100109. [CrossRef]

Disclaimer/Publisher's Note: The statements, opinions and data contained in all publications are solely those of the individual author(s) and contributor(s) and not of MDPI and/or the editor(s). MDPI and/or the editor(s) disclaim responsibility for any injury to people or property resulting from any ideas, methods, instructions or products referred to in the content.